Int. J. Heat Mass Transfer. Vol. 34, No. 8, pp. 1959–1968, 1991
Printed in Great Britain

0017–9310/91 $3.00 + 0.00

Natural convection in a horizontal porous cylinder

LEIV STORESLETTEN
Department of Mathematics, Agder College, 4601 Kristiansand, Norway

and

MORTEN TVEITEREID
Department of Mathematics, Agder College of Engineering, 4890 Grimstad, Norway

(*Received* 30 *August* 1989 *and in final form* 19 *June* 1990)

Abstract—Natural convection in a porous horizontal circular cylinder is considered. The cylinder wall is non-uniformly heated to establish a linear temperature in the vertical direction, with the end sections perfectly insulated. When $L > 0.86$, a unique three-dimensional flow is determined at the onset of convection. For short cylinders ($L < 0.86$) the convection is two-dimensional. In this case there exist two different steady solutions at supercritical Rayleigh numbers, consisting of two and three rolls, respectively. It is proved that both flow structures and any composition of these structures are stable. However, introducing thermal forcing in the applied temperature the flow becomes uniquely determined.

1. INTRODUCTION

THERMAL convection in a saturated porous medium has attracted considerable attention over the last 20 years. This interest in buoyancy induced flow and heat transfer through porous media has been stimulated by several important technical and geophysical applications. We mention applications in geothermal energy recovery [1], extraction of oil and gas from permeable rock reservoirs [2] and radioactive waste heat removal [3].

The present study is concerned with natural convection in a porous medium confined by a horizontal circular cylinder. This problem has been studied by Lyubimov [4]. He considered two different situations of external heating. In one case, when the temperature distribution was linear in the vertical direction, infinitely many stable stationary solutions were found. In the second case, when the temperature was not strictly linear, only one stationary motion was stable. His study is restricted to two-dimensional convection, which seems to be consistent only for short cylinders. Moreover, the paper contains no information about the values of the critical Rayleigh number and the flow patterns occurring for supercritical Rayleigh numbers. We focus, however, our interest on the physical interpretation of the mathematical results, including both two- and three-dimensional convection.

The mathematical formulation of the problem is derived in Section 2. In Section 3 we analyse the marginal stability when the cylinder wall is non-uniformly heated to establish a linear temperature distribution in the vertical direction. For long cylinders there exists a unique three-dimensional steady solution at the onset of convection. For short cylinders, however, it turns out that the convection is two-dimensional. In this case we find two different steady solutions at supercritical Rayleigh numbers. One of the solutions yields a flow pattern consisting of two cells only, whereas the other flow pattern consists of three cells. In Section 4 we apply non-linear analysis to examine the stability of the two different solutions. It is proved that both flow structures are stable. In addition, it also turns out that any composition of these two flows is a stable non-linear solution.

In Section 5 we consider the effect of thermal forcing applied to short cylinders. We employ the theory of singular perturbations of bifurcations described by Matkowsky and Reiss [5] and Tavantzis *et al.* [6]. It is shown that small imperfections, such as thermal forcing in the applied temperature, are sufficient to ensure smooth transition to convection. We also find that the perturbations of the applied temperature uniquely determine the composite non-linear flow and the sign of the circulation.

We notice the hydraulic analogy between the flow in a porous medium and the flow in a narrow gap between parallel vertical walls, i.e. Hele–Shaw cell. Hartline and Lister [7] have shown that the governing equations for convection in a Hele–Shaw cell are the same as the two-dimensional version of the governing equations, given in equations (4). Our investigations concerning short cylinders can therefore be applied to a circular Hele–Shaw cell.

2. GOVERNING EQUATIONS

We consider natural convection in a porous medium confined by a horizontal cylinder of radius r_0 and length L. The porous medium is isotropic,

NOMENCLATURE

A	amplitude
A_n	Fourier coefficients
A_Q, A_S	Landau coefficients
B_n	Fourier coefficients
d	derivative with respect to r, d/dr
g	acceleration of gravity
G_n	Fourier coefficients
H_n	Fourier coefficients
$\mathbf{j}$	vertical unit vector
k	permeability
L	length of the cylinder
m	mode number
N_e	even integer
N_o	odd integer
p	pressure
P_Q, P_S	Landau coefficients
Q	amplitude
r	radial coordinate
r_0	radius of the cylinder
Ra	Rayleigh number, $g\beta\Delta T k r_0/\kappa\nu$
S	amplitude
t	time
T	temperature
T_0	reference temperature
T_b	temperature at the cylinder wall, $T_0 - 1/2\Delta T \sin\phi$
ΔT	characteristic temperature difference
$\mathbf{v}$	velocity
z	horizontal coordinate along the cylinder axis.

Greek symbols

α	wave number
β	coefficient of cubical expansion
γ, δ, ε	small parameters
δ_{in}	Kronecker delta
θ	deviation from static temperature
κ	thermal diffusivity
μ	constant
ν	kinematic viscosity
ϕ	azimuthal coordinate
ψ	stream function.

Subscripts

c	critical values
s	static values.

Superscripts

~	deviation from static values.

homogeneous and saturated by an incompressible fluid. Cylindrical coordinates (r, ϕ, z) are employed with the origin located at one end section, with the z-axis along the axis of the cylinder and the plane $\phi = 0$ being horizontal. The cylinder wall is at a prescribed temperature, given by

$$T_b = T_0 - \tfrac{1}{2}\Delta T \sin\phi \tag{1}$$

while the end sections of the cylinder are perfectly insulated. All boundaries are assumed impermeable. The value of ΔT is taken to be positive so that the medium is heated from below. In Appendix A we have described one situation defining a circumferential temperature as given by equation (1). However, in that specific case, we assumed that no heat exchange took place through the cylinder wall. In the present problem we assume that the heat conductivity of the medium inside the cylinder is small compared to the heat conductivity of the medium (e.g. aluminium) outside the cylinder. In that case equation (1) defines a very good approximation of the cylinder wall temperature.

If ΔT is sufficiently small, the heat transfer in the porous medium will be in the form of conduction. A steady state exists where

$$T = T_s = T_0 - \tfrac{1}{2}\Delta T \frac{r}{r_0}\sin\phi, \quad p = p_s, \quad \mathbf{v} = 0. \tag{2}$$

For larger values of ΔT, in the convective regime, we can write

$$T = T_s + \tilde{\theta}, \quad p = p_s + \tilde{p}, \quad \mathbf{v} = \tilde{\mathbf{v}}. \tag{3}$$

All quantities are now made dimensionless. For example, r, z and L are scaled by the characteristic length r_0.

Invoking the Darcy–Boussinesq approximations the convection is governed by the following equations (the tildes are omitted):

$$\nabla p - Ra\,\theta\mathbf{j} + \mathbf{v} = 0$$

$$\nabla\cdot\mathbf{v} = 0$$

$$\nabla^2\theta + \tfrac{1}{2}\mathbf{v}\cdot\mathbf{j} = \frac{\partial\theta}{\partial t} + \mathbf{v}\cdot\nabla\theta. \tag{4}$$

By eliminating the velocity term on the left-hand side we obtain

$$\nabla^2 p - Ra\left(\sin\phi\frac{\partial}{\partial r} + \cos\phi\frac{1}{r}\frac{\partial}{\partial\phi}\right)\theta = 0$$

$$(\nabla^2 + \tfrac{1}{2}Ra)\theta - \frac{1}{2}\left(\sin\phi\frac{\partial}{\partial r} + \cos\phi\frac{1}{r}\frac{\partial}{\partial\phi}\right)p = \frac{\partial\theta}{\partial t} + \mathbf{v}\cdot\nabla\theta. \tag{5}$$

At the boundaries we have

$$\frac{\partial\theta}{\partial z}=\frac{\partial p}{\partial z}=0, \quad z=0, L$$

$$\theta=\frac{\partial p}{\partial r}=0, \quad r=1. \tag{6}$$

3. MARGINAL STABILITY

The marginal stability problem is defined by the linear version of equations (5) with boundary conditions (6). This linear system is self-adjoint, giving $\partial\theta/\partial t=0$ at the marginal state. The solution can then be expressed by the following Fourier series:

$$p=\left\{\frac{1}{2}A_0+\sum_{n=1}^{\infty}(A_n\cos n\phi+B_n\sin n\phi)\right\}\cos\alpha z$$

$$\theta=\left\{\frac{1}{2}G_0+\sum_{n=1}^{\infty}(G_n\cos n\phi+H_n\sin n\phi)\right\}\cos\alpha z \tag{7}$$

where the Fourier coefficients (amplitudes) are functions of r. To satisfy the boundary conditions at the end sections the wave number α is given by

$$\alpha=\frac{m\pi}{L}, \quad m=0,1,2,\ldots. \tag{8}$$

Introducing expansions (7) into equations (5) and boundary conditions (6), equating terms with the same ϕ-dependence, we get two systems of ordinary differential equations: one for A_n, H_n and the other for B_n, G_n. The system for B_n, G_n is

$$\left(d^2+\frac{1}{r}d-n^2-\alpha^2\right)B_n+\tfrac{1}{2}Ra\left(\left(d+\frac{n+1}{r}\right)G_{n+1}-\left(d-\frac{n-1}{r}\right)G_{n-1}\right)=0$$

$$\left(d^2+\frac{1}{r}d-n^2-\alpha^2+\tfrac{1}{2}Ra\right)G_n-\tfrac{1}{4}\left(\left(d+\frac{n+1}{r}\right)B_{n+1}-\left(d-\frac{n-1}{r}\right)B_{n-1}\right)=0 \tag{9}$$

$$dB_n=G_n=0, \quad r=1. \tag{10}$$

Here $n=0,1,2,\ldots$, $G_{-1}=G_1$ and $B_{-1}=-B_1$. We notice the coordinate singularity at $r=0$. However, the pressure, velocity and temperature are finite single-valued functions, which require at $r=0$:

$$dB_n=dG_n=0, \quad n=0,2,3$$

$$\lim_{r\to 0}\frac{1}{r}B_n=\lim_{r\to 0}\frac{1}{r}G_n=0, \quad n=2,3,4$$

$$\lim_{r\to 0}\left(d-\frac{1}{r}\right)B_1=\lim_{r\to 0}\left(d-\frac{1}{r}\right)G_1=0. \tag{11}$$

Both systems of equations also separate even and odd values of the azimuthal modes. We therefore end up with four independent systems. The coupled amplitudes in each system become:

system I

$$(B_1, B_3, \ldots, G_0, G_2, \ldots)$$

system II

$$(B_2, B_4, \ldots, G_1, G_3, \ldots)$$

system III

$$(A_0, A_2, \ldots, H_1, H_3, \ldots)$$

system IV

$$(A_1, A_3, \ldots, H_2, H_4, \ldots).$$

We have found it convenient to solve the equations by a power series expansion in r. On taking into account conditions (11) the solution of equations (9) for system I may be approximated by the finite series

$$B_n=r^n\sum_{i=0}^{N}c_i\sum_{j=0}^{J}b_{nj}^{(i)}r^{2j}, \quad n=1,3,\ldots,N_o$$

$$G_n=r^n\sum_{i=0}^{N}c_i\sum_{j=0}^{J}g_{nj}^{(i)}r^{2j}, \quad n=0,2,\ldots,N_e. \tag{12}$$

Here N represents the number of terms taken into account in Fourier series (7), and N_o and N_e are odd and even integers, respectively, equal to N or $N-1$. The finite series introduced into equations (9) determine the coefficients $b_{nj}^{(i)}$ and $g_{nj}^{(i)}$ for $j>0$. For $j=0$ the coefficients are set equal to the Kronecker delta δ_{in}. Finally, conditions (10) determine the constants c_i and generate an eigenvalue relation of the form $f(\alpha, Ra)=0$. It turns out by computations that the solution converges rapidly as N and J increase. For a large number of α we have calculated the value of Ra for (N, J) equal to (6, 20) and (9, 30). The difference between the two values of Ra was always less than 10^{-4}.

The four systems of equations, denoted by I, II, III and IV, give four different solutions. The corresponding neutral curves, also denoted by I, II, III and IV, are shown in Fig. 1. The onset of convection is determined by the solution with the lowest Rayleigh number. It follows from the figure that solution I is generated at the onset of convection whenever $\alpha\neq 0$ (three-dimensional convection), whereas both I and II are generated when $\alpha=0$. Solutions III and IV are not generated at the onset of convection for any value of α.

The wave number α is restricted by the relation: $\alpha=m\pi/L$ (equation (8)), where m is the mode number in the direction of the cylinder axis. The value of α at the onset of convection is the one giving the lowest value of the Rayleigh number. This determines the mode number m for a given value of L.

In Fig. 2 we have displayed Ra as a function of L for $m=0, 1, 2,\ldots$ corresponding to solution I in

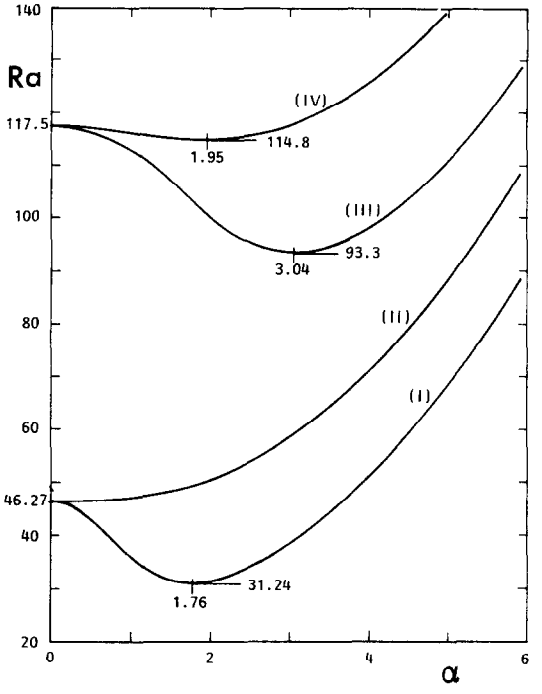

FIG. 1. The four neutral curves corresponding to solutions I, II, III and IV.

Fig. 1. As shown in Fig. 2, the critical mode number for $L \in [0, 0.86]$ is $m = 0$, giving $Ra_c = 46.27$ and $\alpha_c = 0$. In this case the convection is two-dimensional given by solution I or solution II, or a linear combination of these. Moreover, for the range $L \in [0.86, 2.60]$ the critical mode number is $m = 1$. For the range $L \in [2.60, 4.41]$, $m = 2$ and $\alpha = 2\pi/L$, etc.

In the limit of an infinite long cylinder α becomes a free parameter, and the critical values are $Ra_c = 31.24$ and $\alpha_c = 1.76$.

We have found that whenever $L > 0.86$ the onset of convection is three-dimensional and caused by solution I. Moreover, when $L < 0.86$ the convection is two-dimensional and may be composed by any linear combination of solutions I and II. The two-dimensional flow patterns of solutions I and II are shown in Fig. 3. Solution I gives a flow structure of two cells, whereas the structure of solution II consists of three cells.

It is well known in thermal convection problems that the linear equations admit many different solutions [8]. However, by taking into account the non-linear terms the question of pattern may be determined. We shall therefore study the two-dimensional version of equations (4) without cancelling the right-hand side.

4. NON-LINEAR STABILITY ANALYSIS

In this section we shall examine the stability properties of the two- and three-cell structures occurring for short cylinders at slightly supercritical Rayleigh numbers. By taking into account the right-hand side of equations (4), including the non-linear terms, we derive the so-called Landau equations for the problem. This non-linear system of equations will be the basis for our stability analysis.

Since the motion is two-dimensional we introduce the stream function ψ by

$$u = \frac{1}{r}\frac{\partial \psi}{\partial \phi}, \quad v = -\frac{\partial \psi}{\partial r} \tag{13}$$

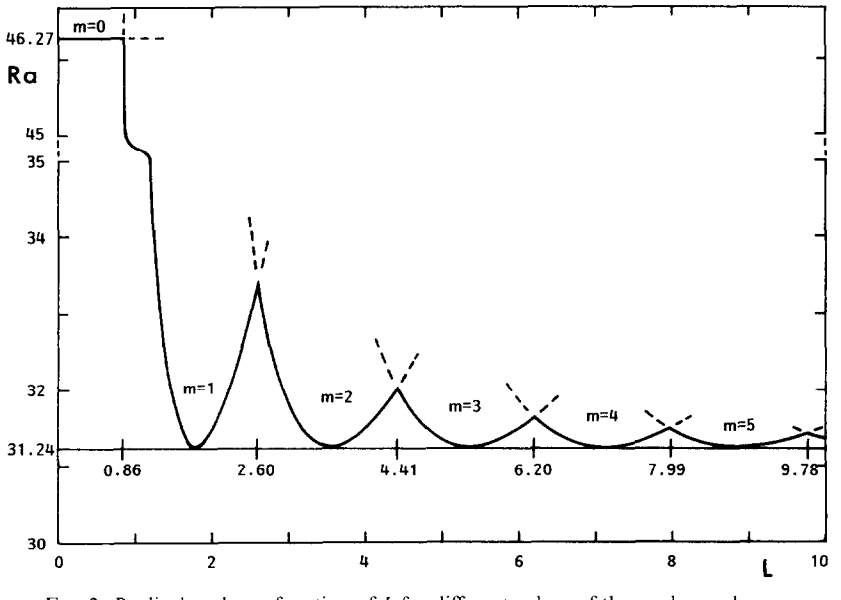

FIG. 2. *Ra* displayed as a function of L for different values of the mode number m.

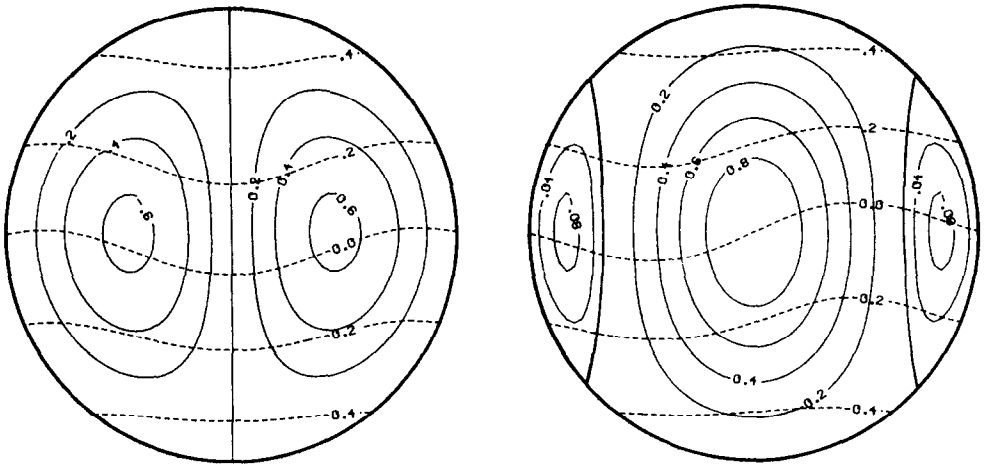

FIG. 3. Computed streamlines (solid) and isotherms (dotted) for solution I (left) and solution II (right).

where u and v are the radial and angular velocity components, respectively. Introducing these expressions into the two-dimensional version of equations (4) we obtain

$$\nabla^2\psi + Ra\left(\frac{\partial\theta}{\partial r}\cos\phi - \frac{1}{r}\frac{\partial\theta}{\partial\phi}\sin\phi\right) = 0$$

$$\nabla^2\theta - \frac{1}{2}\left(\frac{\partial\psi}{\partial r}\cos\phi - \frac{1}{r}\frac{\partial\psi}{\partial\phi}\sin\phi\right) = \frac{\partial\theta}{\partial t} + \mathbf{v}\cdot\nabla\theta \tag{14}$$

with the boundary conditions

$$\psi = \theta = 0 \quad \text{at} \quad r = 1. \tag{15}$$

The solution of equations (14) and (15) can be approximated by the formal expansions

$$\psi = \psi_1 + \psi_2 + \cdots$$

$$\theta = \theta_1 + \theta_2 + \cdots$$

$$Ra = Ra_c + Ra_1 + Ra_2 + \cdots. \tag{16}$$

Moreover, we introduce multiple time scales given by

$$\frac{\partial}{\partial t} = \frac{\partial}{\partial t_1} + \frac{\partial}{\partial t_2} + \cdots. \tag{17}$$

We suppose

$$\psi_i = O(\varepsilon^i) \quad \text{as} \quad \varepsilon \to 0 \tag{18}$$

holds uniformly, and similarly for the other quantities. By introducing expansions (16) and (17) into equations (14) and equating terms of the same order, we find an infinite set of linear equations.

The solutions of the first-order system satisfying boundary conditions (15) may be written as

$$\psi_1 = Q\psi_Q + S\psi_S, \quad \theta_1 = Q\theta_Q + S\theta_S \tag{19}$$

where ψ_Q, θ_Q and ψ_S, θ_S are the solutions found in the linear analysis, corresponding to the two- and three-cell structures, respectively. Here Q and S are amplitudes of order ε.

The operator on the left-hand side of equations (14) is self-adjoint, see Appendix B. Applying the special scalar product (B3) we find the following solvability conditions for the second-order system:

$$Ra_1 = 0, \quad \frac{\partial}{\partial t_1} = 0. \tag{20}$$

The solvability conditions of the third-order system determine Ra_2 and $\partial/\partial t_2$. Neglecting the third-order terms of the expansions for Ra and $\partial/\partial t$, we get the following Landau equations:

$$A_Q\frac{\mathrm{d}}{\mathrm{d}t}Q = \Delta R Q - P_Q(Q^2 + 2Ra_c S^2)Q$$

$$A_S\frac{\mathrm{d}}{\mathrm{d}t}S = \Delta R S - P_S(Q^2 + 2Ra_c S^2)S \tag{21}$$

where $\Delta R = Ra - Ra_c$ and A_Q, A_S, P_Q and P_S are constants calculated to be

$$A_Q = 4.95, \quad A_S = 3.05$$

$$P_Q = P_S = P = 7.66. \tag{22}$$

Equations (21) describe the evolution of the amplitudes due to non-linear interactions.

For subcritical Rayleigh numbers, $\Delta R < 0$, it follows that $Q \to 0$, $S \to 0$ as $t \to \infty$. For supercritical Rayleigh numbers, $\Delta R > 0$, the motionless conduction state $Q = S = 0$ is unstable. However, there exist steady non-zero solutions satisfying

$$Q^2 + 2Ra_c S^2 = \Delta R/P \tag{23}$$

or we may write

$$Q^2 = \frac{\Delta R}{P(1+2Ra_c\,\mu^2)}, \quad S^2 = \frac{\mu^2\Delta R}{P(1+2Ra_c\,\mu^2)}. \tag{24}$$

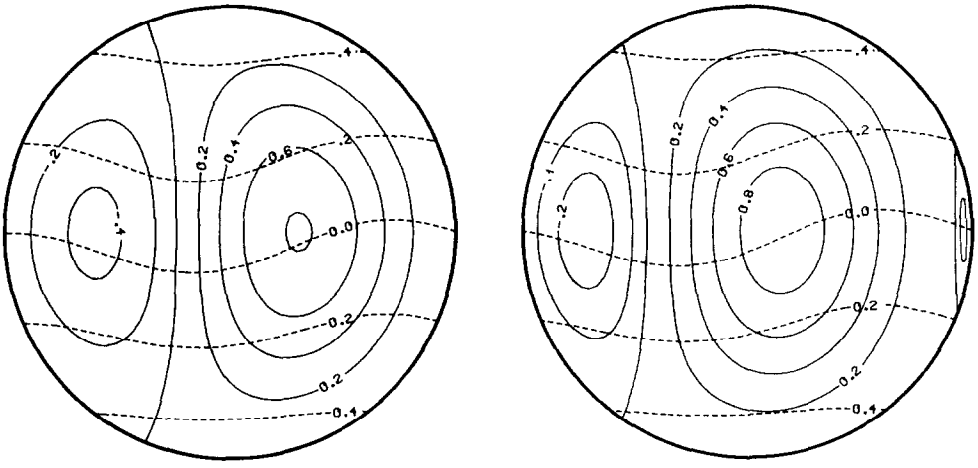

FIG. 4. Computed streamlines (solid) and isotherms (dotted) for the composite solutions corresponding to $2Ra_c\,\mu^2 = 1/3$ (left) and 3 (right).

Here μ^2 may take any value from zero to infinity. The μ^2-values zero and infinity represent the flow patterns consisting of two and three cells, respectively (see Fig. 3). Any other value of μ^2 represents a composition of the two- and three-cell structures. Two different composite flow patterns are shown in Fig. 4.

By considering small perturbations superposed on the steady state solutions (23), it is proved that the solutions are stable for all values of μ. The non-linear analysis therefore fails in selecting a preferred flow pattern. This may be explained by the symmetry of the problem as it appears in the Landau equations ($P_Q = P_S$). Therefore, in order to find a preferred flow one should include other effects, as for example a non-linear term in the momentum equation (non-Darcy fluid) or anisotropy [9]. However, in the next section we shall show that small irregularities of the prescribed temperature at the boundary select a unique value of μ.

In order to draw the bifurcation diagram it is convenient to introduce the amplitude A defined by

$$A^2 = Q^2 + 2Ra_c\,S^2. \tag{25}$$

From equation (23) we obtain

$$A = \pm\sqrt{\left(\frac{\Delta R}{P}\right)}. \tag{26}$$

Thus, according to the non-linear analysis, there is a sharp transition from conduction to convection when the Rayleigh number exceeds the critical value Ra_c. This is a so-called perfect bifurcation, sketched in Fig. 5.

5. SMOOTH TRANSITION BY THERMAL FORCING

In the above section we found that for short cylinders there is a sharp transition from the conduction state to the convection state at $Ra_c = 46.27$, when the temperature at the cylinder wall varied linearly in the vertical direction. However, it is easily shown that for any other applied temperature, the transition to convection occurs smoothly at $Ra_c = 0$. Thermal perturbations of the circumferential temperature may therefore alter the perfect bifurcation at Ra considerably. We are now going to examine these effects. This is of interest, because inaccuracies and different forms of thermal noise are always present in experiments and in applications.

Let $\delta f(\phi)$ represent the temperature perturbation. δ is a small parameter proportional to the magnitude of the noise. It is convenient for the following analysis to expand $f(\phi)$ in a Fourier series. The circumferential temperature is then given by

$$T_b = T_0 - \tfrac{1}{2}\sin\phi + \delta\sum_{n=1}^{\infty}(c_n\cos n\phi + s_n\sin n\phi). \tag{27}$$

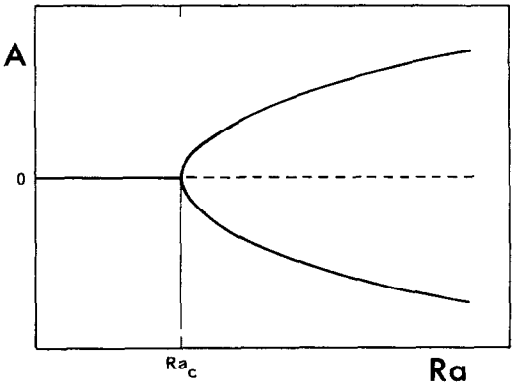

FIG. 5. Sketch of the perfect bifurcation case: ——, stable solution; – – – –, unstable solution.

Here the c_n-terms correspond to the part of the perturbation that is symmetric about the horizontal diameter. The s_n-terms correspond to the asymmetric part. The corresponding quasi-static temperature T_s becomes

$$T_s = T_0 - \tfrac{1}{2}r\sin\phi + \delta\sum_{n=1}^{\infty} r^n(c_n\cos n\phi + s_n\sin n\phi). \quad (28)$$

Substituting for T_s, equations (14) are replaced by

$$\nabla^2\psi + Ra\left(\frac{\partial\theta}{\partial r}\cos\phi - \frac{1}{r}\frac{\partial\theta}{\partial\phi}\sin\phi\right) = -Ra\,\delta\sum_{n=1}^{\infty} nr^{n-1}(c_n\cos(n-1)\phi + s_n\sin(n-1)\phi)$$

$$\nabla^2\theta - \frac{1}{2}\left(\frac{\partial\psi}{\partial r}\cos\phi - \frac{1}{r}\frac{\partial\psi}{\partial\phi}\sin\phi\right) = \frac{\partial\theta}{\partial t} + \mathbf{v}\cdot\nabla\theta + \delta\sum_{n=1}^{\infty} nr^{n-1}\left\{c_n\left(\frac{\partial\psi}{\partial r}\sin n\phi + \frac{1}{r}\frac{\partial\psi}{\partial\phi}\cos n\phi\right) - s_n\left(\frac{\partial\psi}{\partial r}\cos n\phi - \frac{1}{r}\frac{\partial\psi}{\partial\phi}\sin n\phi\right)\right\} \quad (29)$$

which constitute the governing equations for the perturbed problem.

To find steady solutions of equations (29) for values of Ra close to Ra_c, we assume the double expansions

$$(\psi, \theta, Ra) = \sum_{p=0}^{\infty}\sum_{q=0}^{\infty}\varepsilon^p\delta^q(\psi_{pq}, \theta_{pq}, R_{pq}) \quad (30)$$

where ε is the magnitude of the convection amplitude. Notice, however, that the terms with $q = 0$ correspond to the non-linear solutions found in Section 4. The terms with $q \neq 0$ give the modification of those solutions. The equations determining ψ_{01} and θ_{01} are

$$L(\Omega_{01}) = \begin{bmatrix} -Ra_c\sum_{n=1}^{\infty} nr^{n-1}(c_n\cos(n-1)\phi \\ +s_n\sin(n-1)\phi) \\ 0 \end{bmatrix} \quad (31)$$

where L and Ω are defined in Appendix B. The solvability condition of equation (31) requires

$$\sum_{n=1}^{\infty} n\langle\psi_i r^{n-1}(c_n\cos(n-1)\phi + s_n\sin(n-1)\phi)\rangle = 0 \quad (32)$$

where ψ_i represents the ψ_Q- and ψ_S-solutions of Section 4. Conditions (32) are in general not satisfied whenever any $c_n \neq 0$. In that case expansions (30) become invalid as $Ra \to Ra_c$.

On the other hand, if all values of c_n are zero, condition (32) is satisfied for all values of s_n. Expansions (30) converge uniformly to expansions (16) and (17) as $\delta \to 0$. Thus, for small asymmetric perturbations about the horizontal diameter, the solutions of equations (29) are similar to the solutions of equations (14). The perfect bifurcation is replaced by a weakly imperfect bifurcation. The transition remains sharp, but is slightly perturbed.

If there exists $c_n \neq 0$, expansions (30) break down as $Ra \to Ra_c$, and new expansions must be determined. This type of problem has been fully discussed by Matkowsky and Reiss [5] and Tavantzis *et al.* [6], using matched asymptotic expansions. See also Rees and Riley [10]. The appropriate inner expansions are

$$\psi = \gamma\psi_1 + \gamma^2\psi_2 + \gamma^3\psi_3 + \cdots$$
$$\theta = \gamma\theta_1 + \gamma^2\theta_2 + \gamma^3\theta_3 + \cdots$$
$$Ra = Ra_c + \gamma^2 Ra_1 + \gamma^3 Ra_2 + \cdots \quad (33)$$

where $\gamma = \delta^{1/3}$. Moreover, to include the time, we take

$$\frac{\partial}{\partial t} = \gamma^2\frac{\partial}{\partial t_2} + \gamma^3\frac{\partial}{\partial t_3} + \cdots. \quad (34)$$

The problems of order γ and γ^2 are equivalent to the first- and second-order problems considered in Section 4. The $O(\gamma^3)$-equations are

$$L(\Omega_3) = \begin{bmatrix} -Ra_2\,D\theta_1 - Ra_c\sum_{n=1}^{\infty} nr^{n-1}(c_n\cos(n-1)\phi \\ +s_n\sin(n-1)\phi) \\ \frac{\partial\theta_1}{\partial t_2} + \mathbf{v}_1\cdot\nabla\theta_2 + \mathbf{v}_2\cdot\nabla\theta_1 \end{bmatrix}. \quad (35)$$

The solvability conditions of equation (35) give two equations for Ra_2 in terms of Q, S, $\partial Q/\partial t_2$ and $\partial S/\partial t_2$. Omitting the details, the amplitude equations of the problem now become

$$A_Q\frac{\mathrm{d}}{\mathrm{d}t}Q = \Delta RQ - P(Q^2 + 2Ra_c S^2)Q + b_Q$$
$$A_S\frac{\mathrm{d}}{\mathrm{d}t}S = \Delta RS - P(Q^2 + 2Ra_c S^2)S + b_S. \quad (36)$$

Here A_Q, A_S and P are the same coefficients as in Section 4, and

$$b_Q = Ra_c\,\delta\langle\psi_Q\Sigma nr^{n-1}c_n\cos(n-1)\phi\rangle$$
$$b_S = Ra_c\,\delta\langle\psi_S\Sigma nr^{n-1}c_n\cos(n-1)\phi\rangle. \quad (37)$$

We notice that the $s_n\sin n\phi$ terms do not effect the values of b_Q and b_S at $O(\delta)$. We may therefore, without loss of generality, exclude asymmetric perturbations about the horizontal diameter.

5.1. *Discussions of the steady solutions*

The amplitude equations (36) describe the evolution of the amplitudes Q and S due to non-linear interactions for ΔR of order $\delta^{2/3}$. We consider arbitrary temperature perturbations, which generally

imply that $b_Q \neq 0$ and $b_S \neq 0$. The amplitude equations then yield the following steady-state solutions:

$$S = \mu Q \tag{38}$$

where

$$\mu = b_S/b_Q \tag{39}$$

and

$$P(1+2Ra_c\,\mu^2)Q^3 - \Delta R Q - b_Q = 0. \tag{40}$$

This results in one, two or three solutions for S and Q as Ra is less than, equal to, or greater than Ra_1, where

$$Ra_1 = Ra_c + \tfrac{3}{2}\{2P(1+2Ra_c\,\mu^2)b_Q^2\}^{1/3}. \tag{41}$$

We define the amplitude

$$A = \sqrt{(1+2Ra_c\,\mu^2)}\,Q \tag{42}$$

which is consistent with equation (25). By solving Q from equation (40) with b_Q positive we get the solutions for A as shown in Fig. 6. A negative value of b_Q reflects the solutions about the Ra-axis.

By standard methods it is easily proved that the positive branch is stable for all μ. The negative branches for $Ra \geqslant Ra_1$ are, however, unstable.

Considering $|\Delta R| \to \infty$ in equation (40), we find that the solutions are matched asymptotically to the solutions found in Section 4. The positive branch approaches $\sqrt{(\Delta R/P)}$, and the lower negative branch approaches $-\sqrt{(\Delta R/P)}$ (see equation (26)). Moreover, the zero-solution is approached by the positive branch as $\Delta R \to -\infty$, and by the upper negative branch as $\Delta R \to \infty$.

We notice that the perturbations of the circumferential temperature have changed the bifurcation dramatically. Figure 6 shows no sharp transition, as Fig. 5, from conduction to convection at $Ra = Ra_c$, but a smooth transition at $Ra = 0$. The perturbations result in a so-called imperfect bifurcation. Another important feature is that the amplitudes Q and S now become fully determined by ΔR, b_Q and b_S. This is in contrast to the perfect bifurcation case where α could take any real value, giving an infinite number of steady solutions.

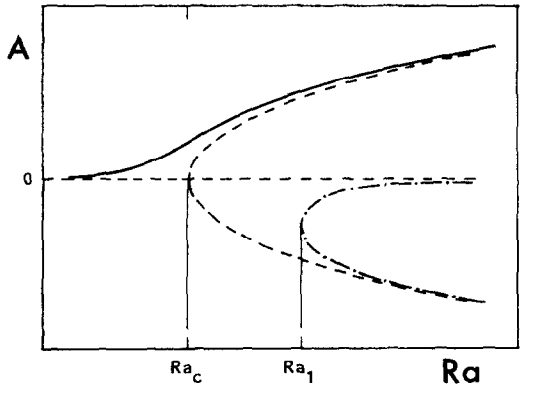

FIG. 6. Sketch of the imperfect bifurcation case: ——, stable solution; – · – · –, unstable solution; – – –, perfect bifurcation curves.

Finally, we turn to the question of preferred flow pattern for two special types of perturbations, giving imperfect bifurcation. The perturbations of the applied temperature can be divided into symmetric and asymmetric parts about the vertical diameter, consisting of even and odd $\cos n\phi$ terms, respectively. From equations (37) it follows that the symmetric perturbations give $b_S = 0$, whereas symmetric perturbations give $b_Q = 0$. Furthermore, from equations (38) to (40) it follows that $S = 0$ and $Q \neq 0$, when $b_S = 0$. When $b_Q = 0$, we easily find that $Q = 0$ and $S \neq 0$. Therefore, when the perturbations are symmetric about the vertical diameter, the flow consists of the symmetric two-cell pattern. For asymmetric perturbations the flow consists of the symmetric three-cell pattern. These types of flow are shown in Fig. 3.

6. SUMMARY

In the present paper we have considered natural convection in a saturated porous medium confined by a horizontal circular cylinder. The cylinder wall is non-uniformly heated to establish a linear temperature distribution in the vertical direction, and the appropriate temperatures are assumed to be maintained on the walls at all times.

The analysis indicates that the critical Rayleigh number Ra_c and the corresponding wave number α_c depend on the length L of the cylinder. The results are displayed in Fig. 2 which gives Ra_c as a function of L. For long cylinders the convection is three-dimensional. For a short cylinder ($L < 0.86$), however, the onset of convection occurs at $Ra_c = 46.27$ and $\alpha_c = 0$, which means that the convection is two-dimensional. Moreover, in this case the conduction state bifurcates into two qualitatively different convective solutions. One of the solutions gives a symmetric flow pattern consisting of two counter-rotating rolls. The flow of the second solution consists of three rolls. In order to follow the solutions into the supercritical regime we have derived the Landau equations of the problem. It follows that both solutions are stable solutions of the corresponding non-linear problem. We also find that any linear composition of these two solutions is a stable solution.

In experiments and in real applications the sharp transition rarely occurs. Usually one observes that the transition occurs smoothly. Imperfections, impurities or other inhomogeneities tend to distort the transition. We have studied these effects by considering small perturbations (thermal forcing) superposed the temperature of the cylinder wall. In the case that the perturbations are not asymmetric about the horizontal diameter of the cylinder, the transition is changed dramatically. The transition now emanates smoothly from $Ra = 0$. Moreover, the corresponding

non-linear flow turns out to be uniquely determined. On the other hand, when the perturbations are asymmetric about the horizontal diameter, we find that the perturbations modify, but do not destroy the sharp transition. This is a so-called weak imperfection case. However, since thermal noise is arbitrary and always present in experiments, it is unlikely that weak imperfect or perfect bifurcation will be observed. We would expect smooth transition in experiments of the present problem.

Acknowledgements—The authors are grateful to Dr D. S. Riley, University of Bristol, for having directed their attention to the problem investigated in this paper and for valuable discussions.

REFERENCES

1. P. Cheng, Heat transfer in geothermal systems, *Adv. Heat Transfer* **14,** 1–105 (1978).
2. M. Combarnous and K. Aziz, Influence de la convection naturelle dans les d'huile ou de gaz, *Revue Inst. Fr. Pétrole* **25,** 1335–1353 (1970).
3. J. Bear, *Dynamics of Fluids in Porous Media*. American Elsevier, New York (1972).
4. D. V. Lyubimov, Convective motions in a porous medium heated from below, *Zh. Prikl. Mekh. Tekh. Fiz.* No. 2, 131–137 (1975); *J. Appl. Mech. Tech. Phys.* **16,** 257–261 (1975).
5. B. J. Matkowsky and E. L. Reiss, Singular perturbations of bifurcations, *SIAM J. Appl. Math.* **33,** 230–255 (1977).
6. J. Tavantzis, E. L. Reiss and B. J. Matkowsky, On the smooth transition to convection, *SIAM J. Appl. Math.* **34,** 322–337 (1978).
7. B. K. Hartline and C. R. B. Lister, Thermal convection in a Hele–Shaw cell, *J. Fluid Mech.* **79,** 379–389 (1977).
8. E. Palm, Nonlinear thermal convection, *Ann. Rev. Fluid Mech.* **7,** 39–61 (1975).
9. T. Nilsen and L. Storesletten, An analytical study on natural convection in isotropic and anisotropic porous channels, *ASME J. Heat Transfer* **112,** 396–401 (1990).
10. D. A. S. Rees and D. S. Riley, Free convection in an undulating saturated porous layer: resonant wavelength excitation, *J. Fluid Mech.* **166,** 503–530 (1986).

APPENDIX A. THE CIRCUMFERENTIAL TEMPERATURE

To establish the prescribed temperature

$$T_b = T_0 - \tfrac{1}{2}\Delta T \sin\phi \tag{A1}$$

at the boundary of the cylinder, we consider the steady-state conduction in a large plate with a circular hole of radius r_0. Let (x, y) be Cartesian coordinates with the origin at the centre of the hole. Moreover, (r, ϕ) denote polar coordinates with the line $\phi = 0$ along the x-axis and $r^2 = x^2 + y^2$. We want to find the temperature of the plate under the following conditions: no heat exchange takes place with the hole; no heat conduction in the direction normal to the plate; at large values of r the heat is conducted in the y-direction, only. The system to be solved, giving $T = T_b$ at $r = r_0$, is then

$$\left(\frac{\partial^2}{\partial x^2} + \frac{\partial^2}{\partial y^2}\right) T = 0, \quad r > r_0$$

$$\frac{\partial T}{\partial r} = 0, \quad r = r_0$$

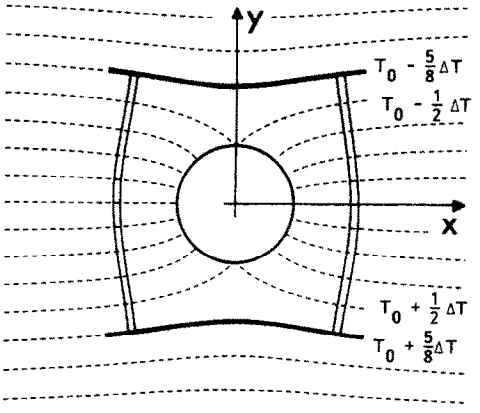

FIG. A1. The temperature distribution of the plate outside the hole of radius r_0. The dashed curves represent the isotherms. The temperature difference is equal to $\frac{1}{8}\Delta T$ between each pair of neighbouring isotherms. The solid lines at $T_0 \pm \frac{5}{8}\Delta T$ represent boundaries of constant temperature. The double lines normal to the isotherms represent insulated boundaries.

$$\frac{\partial T}{\partial x} \to 0, \quad \frac{\partial T}{\partial y} \to -\frac{\Delta T}{4r_0}, \quad r \to \infty. \tag{A2}$$

The solution is

$$T = T_0 - \frac{\Delta T}{4r_0}\left(1 + \frac{r_0^2}{x^2 + y^2}\right) y \tag{A3}$$

or in polar coordinates

$$T = T_0 - \frac{\Delta T}{4r_0}\left(1 + \frac{r_0^2}{r^2}\right) r \sin\phi. \tag{A4}$$

The temperature distribution of the plate is shown in Fig. A1. The same temperature distribution may also be achieved in a plate of finite extent. For example, as illustrated in Fig. A1, by introducing boundaries of constant temperature along two isotherms and insulated boundaries normal to the isotherms.

APPENDIX B. SELF-ADJOINTNESS OF EQUATION (14)

The left-hand side of equation (14) may be written as

$$\begin{bmatrix} \nabla^2 & Ra\, D \\ -\tfrac{1}{2}D & \nabla^2 \end{bmatrix} \begin{bmatrix} \psi \\ \theta \end{bmatrix} = L(\Omega) = 0 \tag{B1}$$

where

$$D = \cos\phi \frac{\partial}{\partial r} - \sin\phi \frac{1}{r}\frac{\partial}{\partial \phi}. \tag{B2}$$

Let Ω' and Ω'' be any functions which satisfy the same boundary conditions as Ω. We define the scalar product

$$\{\Omega', \Omega''\} = \langle \psi' \psi'' \rangle + 2Ra \langle \theta' \theta'' \rangle \tag{B3}$$

where $\langle\ \rangle$ is the average over the entire volume, i.e.

$$\langle(\ )\rangle = \frac{1}{2\pi}\int_0^1 \int_0^{2\pi} (\ )\, d\phi\, r\, dr. \tag{B4}$$

Then the operator L has the following property of self-adjointness:

$$\{\Omega', L(\Omega'')\} = \{\Omega'', L(\Omega')\}. \tag{B5}$$

CONVECTION NATURELLE DANS UN CYLINDRE POREUX HORIZONTAL

Résumé—On considère la convection naturelle dans un cylindre horizontal à section circulaire et poreux. La paroi du cylindre est chauffée de façon non uniforme pour créer une température linéaire dans la direction verticale, avec les sections terminales parfaitement isolées. Quand $L > 0{,}86$, un écoulement unique tridimensionnel est déterminé au début de la convection. Pour des cylindres courts ($L < 0{,}86$) la convection est bidimensionnelle. Dans ce cas il existe deux solutions permanentes différentes aux nombres de Rayleigh supercritiques, consistant respectivement en deux et trois rouleaux. On prouve que les deux structures d'écoulement et une composition quelconque de ces structures sont stables. Néanmoins, en introduisant un forçage thermique dans la température appliquée, l'écoulement devient déterminé de façon unique.

NATÜRLICHE KONVEKTION IN EINEM WAAGERECHTEN PORÖSEN ZYLINDER

Zusammenfassung—Die natürliche Konvektion in einem porösen waagerechten Kreiszylinder wird betrachtet. Um eine lineare Temperaturverteilung in senkrechter Richtung zu erreichen, wird die Zylinderwand ungleichförmig beheizt; die Stirnflächen des Zylinders sind adiabat. Für $L > 0{,}86$ ist die Strömung beim Einsetzen der Konvektion dreidimensional, für kurze Zylinder ($L < 0{,}86$) zweidimensional. In diesem Fall existieren bei überkritischen Rayleigh-Zahlen zwei unterschiedliche stationäre Lösungen mit zwei bzw. drei Konvektionswalzen. Es zeigt sich, daß beide Strömungsformen und beliebige Mischformen stabil sind. Wenn jedoch eine treibende Temperatur aufgeprägt wird, erhält man eine eindeutige Lösung.

ЕСТЕСТВЕННАЯ КОВЕКЦИЯ В ГОРИЗОНТАЛЬНОМ ЦИЛИНДРЕ ИЗ ПОРИСТОГО МАТЕРИАЛА

Аннотация—Исследуется естественная конвекция в горизонтальном круговом цилиндре из пористого материала. Стенка цилиндра неравномерно нагревается, так что устанавливается линейное распределение температуры в вертикальном направлении, в то время как торцевые поверхности полностью изолированы. При $L > 0{,}86$ после возникновения конвекции имеет место однозначное решение в виде трехмерного течения. В случае цилиндров малой длины ($L < 0{,}86$) конвекция является двумерной, причем для закритических чисел Рэлея сущехтвуют два различных стационарных решения, состоящих соответственно из двух и трех валов. Доказано, что обе структуры течения и любая их композиция являются устойчивыми. Однако при внешнем тепловом воздействии течение определяется однозначно.